

GAP FLOW AND VERTICAL MIXING AT THE SOUTHERN END OF THE GSL BASIN

J. O. Pinto^{1,2,*}, D. B. Parsons², W. O. J. Brown², S. Cohn², N. Chamberlain², and B. Morley²

¹University of Colorado, Boulder, Colorado

²National Center for Atmospheric Research, Boulder, CO

Introduction

The VTMX (Vertical Transport and Mixing) field experiment took place in 3-25 October 2000 in the Great Salt Lake Basin (<http://www.pnl.gov/VTMX/>).

It was designed to observe the processes that lead to vertical transport and mixing under stable conditions in complex terrain. As part of the field experiment, measurements were made by NCAR with an Enhanced Boundary Layer ISS (EBLISS) at the southern end of the Great Salt Lake (GSL) Basin to characterize the flow between the GSL Basin and the Utah Lake Basin (see *Pinto et al.* 2002 for more details). When the wind is from the south, it is channeled through Jordan Gap causing it to accelerate. Under conditions of weak synoptic forcing at night, a pressure gradient sets up between and within the two basins resulting in down-valley flow in the GSL Basin also resulted in “gap flow” as described by *Whiteman* (2000). Gap flow was observed at the NCAR site more than 50% of the time during the three week period and occurred under a variety of synoptic regimes.

In this paper we discuss the characteristics of gap flow and how it affected vertical mixing in the southern end of the GSL Basin.

Instrumentation

The NCAR deployed an Enhanced Boundary Layer ISS (EBLISS) at the southern end of the Great Salt Lake Basin as part of the Vertical Transport and Mixing Field Experiment. The site was instrumented with a suite of in situ and remote sensing platforms that allowed near continuous monitoring of the boundary layer. Components of the EBLISS deployed for VTMX included:

- 2 surface observing stations
- GLASS radiosondes
- Tethered Atmospheric Observing System (TAOS)
- METEK mini-sodar

- Multiple Antenna Profiling Radar (MAPR)
- Scanning Aerosol Backscatter Lidar (SABL)

Atmospheric soundings and tethered balloon operations occurred during IOPs while operation of the remote sensing instruments was nearly continuous. This was the first deployment of the TAOS platform and it performed well. Data were typically collected by five sondes tethered between 75 and 600 m during the IOPs. The sodar also performed well, providing wind measurements up to 400 m. SABL proved very useful for determining boundary layer depth and vertical layering. Unfortunately, SABL experienced several hardware failures that limited the quality of the data at times. The MAPR wind profiler experienced signal to noise problems throughout the experiment due to the dry conditions and the migration of birds. More details of the NCAR deployment may be found at: <http://www.atd.ucar.edu/r/f/projects/vtmx/>.

Gap Flow Characteristics

The timing, duration, strength, and depth of each gap flow event observed during VTMX is listed in Table 1. The gap flow was intermittent on several instances as seen in Figure 1. The depth of the gap flow is determined using wind data collected with the sodar, TAOS, and radiosondes. The strength of the flow is indicated by the peak 5-min average wind speed at 10 m. It was found that the strongest winds typically occurred below 200 m.

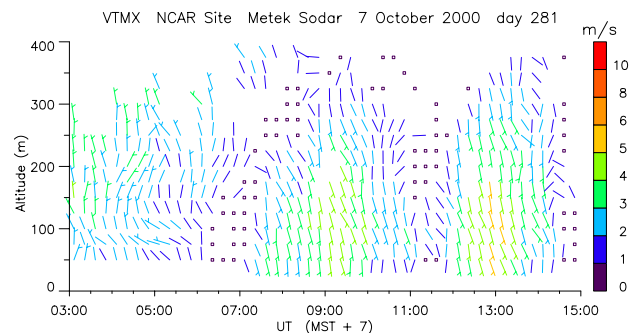


Figure 1. Sodar wind speed and direction obtained on 07 October 2000.

* Corresponding author address: Dr. James O. Pinto, NCAR, P.O. Box 3000, Boulder, CO, 80307-3000, email: pinto@ucar.edu

Vertical mixing associated with the gap flow is evident in Figure 2. The vertical velocity variance significantly increased after onset of the gap flow with a particularly strong up-down couplet evident between 0815 and 0900 UTC. These strong vertical motions and enhanced turbulence acted to mix relatively warm air downward and cold air upward effectively reducing the local stability (Figure 3). The heating due to vertical mixing can be estimated if we know the radiative cooling rate and if we assume that contributions from horizontal advection are small. Prior to onset of the gap flow the observed decrease in temperature can be related to the radiative cooling rate estimated with a two-stream radiative transfer model (Figure 4). Just two hours after onset, the residual is as large as 4 K just above the surface where the coldest air is being replaced by the warmer air from above.

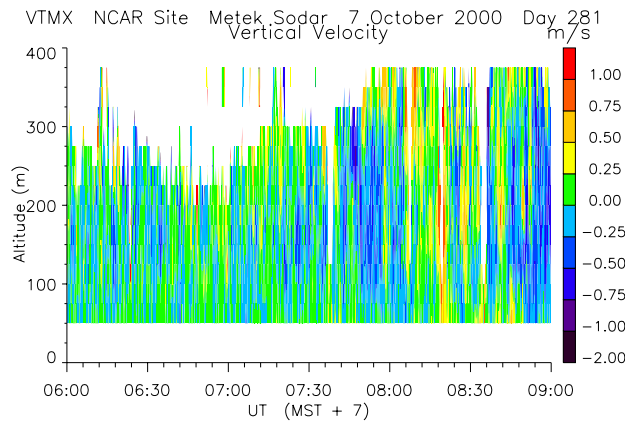


Figure 2. Raw vertical velocity obtained with the minisodar. Gap flow began at 0700 UTC as seen in figure 1.

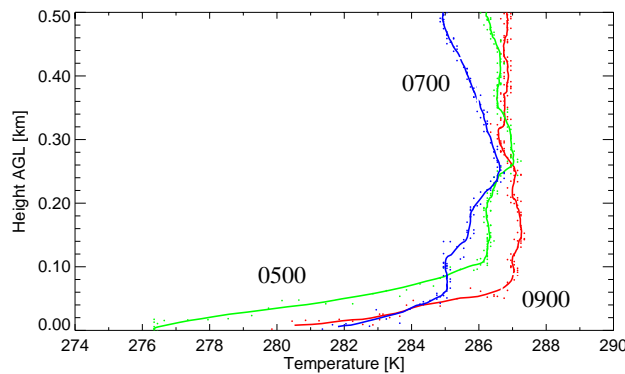


Figure 3. Sequence of three soundings obtained at 0500, 0700 and 0900 UTC on October 7.

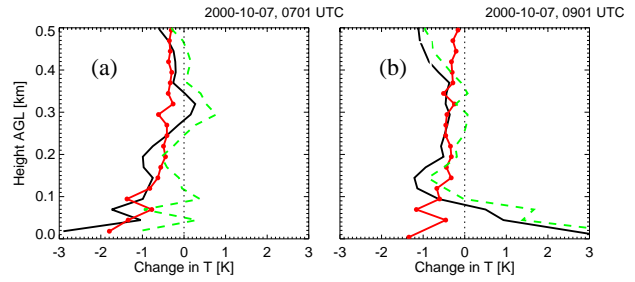


Figure 4. The change in temperature observed between (a) 0500 and 0700 UTC and (b) 0700 and 0900 UTC (solid line). Also shown is the change in temperature due to radiative cooling (connected dots) and the difference between the observed change and the change due to radiative cooling or the residual (dashed line).

Table 1. Gap flow Characteristics

Date	Start/Endtime, UTC	Depth, m	Strength*, m s ⁻¹
10-4	0400-1600	300+	2.0
10-6	0500-1930	300+	3.0
10-7	0600-1500	380	1.2
10-8	1015-1500	100	0.7
10-9	0430-0000	1250	4.8
10-15	0415-2215	940	3.3
10-16	0415-2230	400+	4.7
10-17	0430-2200	1130	4.0
10-18	0400-0100	760	5.3
10-19	0400-1800	400+	5.6
10-20	0415-1500+	810	1.8
10-24	0430-0000	400+	4.5
Avg, N=12	0500-2015	100-1250	3.4

*mean wind speed at 10 m during gap flow event

Modeling

Modeling studies are being conducted to better understand the processes which determine the characteristics of the gap flow and the strength and duration of vertical mixing associated with them. Here, we employ the NCAR/Penn State mesoscale model (MM5) using two different resolutions to demonstrate problems with the treatment of weakly forced flow in complex terrain, such as that observed on October 7. Several circulations that developed during the night on October 7 were simulated, including down-valley flow, katabatic flow, drainage winds down the canyons and gap flow.

Here, we focus on the gap flow observed at the southern end of the GSL Basin. Using the v-wind component as an indicator, it is seen that the onset of the gap flow is well simulated (Figure 6), but that its depth and duration are overpredicted at both resolutions. Interestingly, this problem is exacerbated in the simulation with increased horizontal resolution (Figure 5).

Errors in the simulation of gap flow depth and duration may be partly attributable to the treatment of the stable boundary layer in the complex terrain. As discussed by *Bader et al.* (1989), there are several difficulties in representing the horizontal variability in vertical structure and depth of stable boundary layers in complex terrain, not the least of which is the assumption of horizontal homogeneity that is made in many boundary layer schemes (e.g., *Blakadar*, 1979).

Acknowledgments. We would like to thank the DOE EMP program for financial support of this project. Conversations with C. Doran have also been helpful in directing the focus of our studies and planning of future field campaigns.

Pinto, J.O., D.B. Parsons, W.O.J. Brown, B. Morley, N. Chamberlain, and S. Cohn, 2002: Vertical mixing associated with thermally-driven flow at the southern end of the Great Salt Lake Basin, to be submitted to *Bull. Amer. Meteor. Soc.*
 Whiteman, C.D., 2000: *Mountain Meteorology: Fundamentals and Applications*. Oxford University Press, Inc., New York, New York. 355 pp.

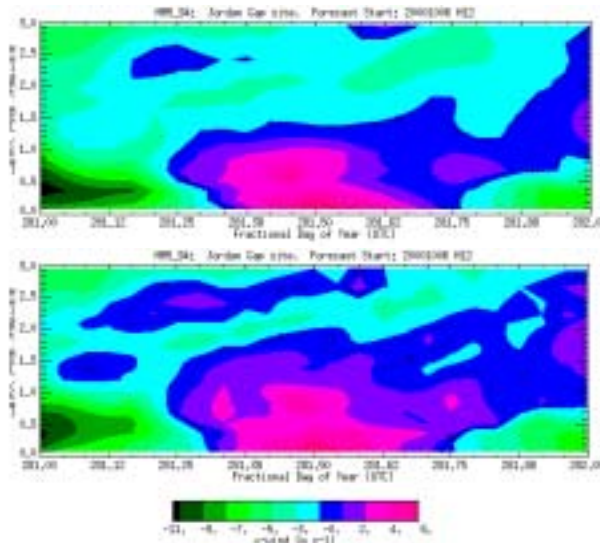


Figure 5. Analysis of the v-wind for simulations of the gap flow observed on 07 Oct 2000 (day 281) for horizontal resolutions of (a) 3.0 and (b) 1.0 km.

References

Bader, D.C., T.B. McKee, and G.J. Tripoli, 1987: Mesoscale boundary-layer evolution over complex terrain, Part 1: Numerical simulation of the diurnal cycle. *J. Atmos. Sci.*, 44, 2823-2838.
 Blackadar, A.K., 1979: High resolution models of the planetary boundary layer. *Adv. Environ. Sci. Eng.*, 1, 50-85.